Proportional Joint-Moment Control for Instantaneously Adaptive Ankle Exoskeleton Assistance

Gian Maria Gasparri, Jason Luque, and Zachary F. Lerner

***Abstract*— Lower-limb exoskeletons used to improve free-living mobility for individuals with neuromuscular impairment must be controlled to prescribe assistance that adapts to the diverse locomotor conditions encountered during daily life, including walking at different speeds and across varied terrain. The goal of this paper is to design and establish clinical feasibility of an ankle exoskeleton control strategy that instantly and appropriately adjusts assistance to the changing biomechanical demand during variable walking. To accomplish this goal, we developed a proportional joint-moment control strategy that prescribes assistance as a function of the instantaneous estimate of the ankle joint moment and conducted a laboratory-based feasibility study. Four individuals with neuromotor impairment and one unimpaired individual completed exoskeleton-assisted slow and fast gait transition tasks that involved gait initiation and changing walking speed. We found that the controller was effective in instantaneously prescribing exoskeleton assistance that was proportional to the ankle moment with less than 14% root-mean-square error, on average. We also performed a three-subject pilot investigation to determine the ability of the proportional joint-moment controller to improve walking economy. Evaluated in two individuals with cerebral palsy and one unimpaired individual, metabolic cost of transport improved 17–27% during treadmill and over-ground walking with proportional control compared with wearing the exoskeleton unassisted. These preliminary findings support the continued investigation of proportional joint-moment control for assisting individuals with neuromuscular disabilities during walking in real-world settings.**

***Index Terms*— Gait, walking, wearable robotics, rehabilitation robotics, metabolic cost.**

I. Introduction

IMPAIRMENT of the human neuromuscular system, including from stroke, Parkinson's disease, and cerebral palsy (CP), often leads to lower-extremity impairment and significantly reduced long-term mobility [1]–[4]. Despite conventional treatments and walking aids, nearly all affected individuals fail to attain normal function and activity levels [5], [6]. Advances in actuators, power storage, and computing have led to the design and implementation of robot-assisted therapy and mobility. Exoskeletons designed to increase mobility primarily augment the ankle joint because proper ankle function is essential for efficient bipedal walking [7], [8], while neuromuscular impairment affecting the lower-extremity typically results in reduced ankle push-off during mid-late stance [3], [9]. However, current ankle exoskeletons have exhibited limited or no benefit outside of controlled laboratory environments, with effective control a primary limiting factor.

The control of lower-limb exoskeletons to augment or restore mobility in real-world settings for individuals with neuromuscular impairment remains a critical challenge in the field of wearable robotics. Exoskeleton control strategies capable of improving mobility must adapt to the diverse locomotor conditions encountered during daily life, such as gait initiation, and walking at different speeds and across varied terrain. Additionally, in order for wearable robotic devices to be successfully adopted into daily life, their control strategies must be robust to user and environmental variability, allow for self-implementation, and maximize ease of use.

A variety of control strategies have been developed for exoskeletons across a number of walking conditions, yet several limitations exist for their practical or clinical implementation in real-world settings. Phase variable control [10] has demonstrated promising results during variable walking speed [11] and stair climbing [12], but requires more research to demonstrate effectiveness and reliability for individuals with irregular, asymmetric, and changing gait patterns. Measurement of muscle activity (electromyography, (EMG)) signals have been used to distinguish ambulatory conditions [13], and for proportional myoelectric control with great success in unimpaired individuals [14], [15]. In clinical populations such as CP, muscle spasticity can saturate the volitional neuromuscular control in the EMG pattern [16]. Furthermore, EMG control relies on, and is susceptible to, changes in electrode-skin conductivity, motion artifact, electrode placement, fatigue, and cross-talk [17], [18]; these challenges may pose realistic barriers for using proportional myoelectric control during daily life. The use of human in the loop optimization [19], while successful in unimpaired individuals walking in controlled settings (i.e. treadmill or stair stepper at set speeds), requires relatively lengthy learning periods (120+ minutes), and is not yet suited for adapting to instantaneous changes locomotor

Manuscript received November 30, 2018; revised January 15, 2019 and March 1, 2019; accepted March 11, 2019. Date of publication March 19, 2019; date of current version April 8, 2019. This work was supported in part by NSF under Grant 1756029 and in part by the Arizona Department of Health Services under Grant ADHS18-198864. *(Corresponding author: Zachary F. Lerner.)*

G. M. Gasparri and J. Luque are with the Mechanical Engineering Department, Northern Arizona University, Flagstaff, AZ 86011 USA.

Z. F. Lerner is with the Mechanical Engineering Department, Northern Arizona University, Flagstaff, AZ 86011 USA, and also with the Department of Orthopedics, The University of Arizona College of Medicine–Phoenix, Phoenix, AZ 85004 USA (e-mail: zachary.lerner@nau.edu).

This paper has supplementary downloadable material available at http://ieeexplore.ieee.org, provided by the author.

Digital Object Identifier 10.1109/TNSRE.2019.2905979

TABLE I
PARTICIPANT INFORMATION

Participant	Condition	Age (yrs)	Gender	Height (m)	Body Mass (kg)	Preferred Speed (m/s)	Nominal Torque (Nm/kg)
CP_1	CP, GMFCS I	30	M	1.70	51.0	1.05	14
CP_2	CP, GMFCS I	12	M	1.39	34.8	0.95	12
CP_3	CP, GMFCS III	22	F	1.47	45.3	0.55	12
P_4	PD, H-Y II	85	F	1.51	46.5	0.80	10
U_5	Unimpaired	21	F	1.60	52.3	1.10	16

CP: Cerebral Palsy. GMFCS: Gross Motor Function Classification System. PD: Parkinson's disease. H-Y: Hoehn and Yahr stage.

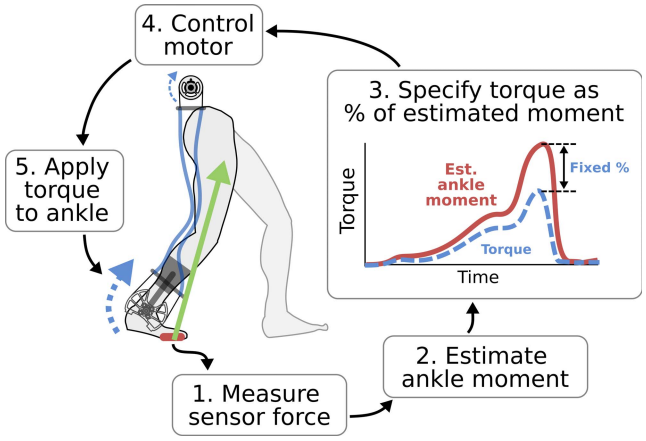

Fig. 1. Proportional joint-moment control. A method for prescribing exoskeleton assistance that is proportional to the ankle joint moment.

condition. Implementation of control algorithms for intent recognition and activity classification during walking, sitting, standing, and stair climbing [20]–[22] in clinical populations is possible but remains challenging because of potential gait variability and progressive ambulatory deterioration. The inability or failure to detect completely unique conditions (e.g. irregular walking, stumbling, unforeseen obstacles, unexpected disturbances, etc.) could have dangerous consequences.

The purpose of this paper was to develop and evaluate an ankle exoskeleton control scheme that (1) automatically adapts assistance across locomotor tasks encountered during daily life, (2) is well-suited for assisting individuals with pathological gait patterns, and (3) is realistic to implement in real-world settings. First, we conceptualized a novel control strategy based on the concept of providing assistance that is proportional to the instantaneous demand placed on the ankle joint (Fig. 1). Next, we designed and calibrated a custom sensing mechanism necessary to estimate the ankle moment in real-time. Finally, we conducted a validation and clinical feasibility study in ambulatory individuals with neuromotor impairment from CP (n = 3) and Parkinson's Disease (n = 1), and in one unimpaired individual. The primary objective of the validation study was to evaluate the performance of the control strategy during gait initiation and variable walking. Additionally, because a primary goal of wearable assistance is to improve walking efficiency, a secondary objective of this work was to provide a preliminary assessment of the ability of the control strategy to reduce the energy cost of both treadmill and over-ground walking. This study lays the foundation for an adaptive exoskeleton control strategy that is suitable for clinical populations and is designed to maximize usability across a wide range of user ages, cognitive abilities, and fine motor skills. Additional detail on the novel contribution of the present study relative to our prior clinically-focused work can be found in Supplemental Table I.

II. METHODS

A. Proportional Joint-Moment Control Theory

Our novel control strategy – *Proportional Joint-Moment Control* – is based on the concept of providing assistance that is proportional to the instantaneous demand placed on a biological joint (i.e. the net moment generated by muscles and other biological tissues crossing a joint). This approach requires estimating the user's joint moment in real-time and prescribing assistance as a fixed percentage. We theorized that exoskeleton torque that is instantaneously synchronized with the net muscular demand at a joint will intuitively and safely capture the user's intention.

B. Ankle Moment Estimation

We developed an approach to estimate the ankle joint moment in real-time based on the theory of a simple torque balance (Fig. 2A). We approximated the torque produced by the ankle muscles (net muscle moment) by balancing the resultant torque produced by the ground reaction force. High-range force sensors (FlexiForce A201, Tekscan) located under the forefoot were used to approximate the ground reaction force, along with an inferred point of force application (center of pressure).

Sensor calibration and mapping was completed by having one unimpaired individual walk wearing the ankle exoskeleton without assistance across a varying speed profile on a treadmill while we collected gait kinematics and kinetics. In three separate acceleration trials (0.25, 0.125, and 0.083 m/s^2), the treadmill increased speed from 0 m/s to 1.25 m/s, then, following 10 seconds at constant speed, decreased to 0 m/s. Gait analysis and biomechanical modeling was completed as described in Section II.F, below, to compute the biological ankle moment via inverse dynamics. We analyzed several sensor placement locations. The arrangement that resulted in the greatest prediction accuracy included a sensor placed directly under the head of the 1st metatarsal bone (location "A" in Fig. 2A) and another placed along the path of the center of pressure (location "B" in Fig. 2A).

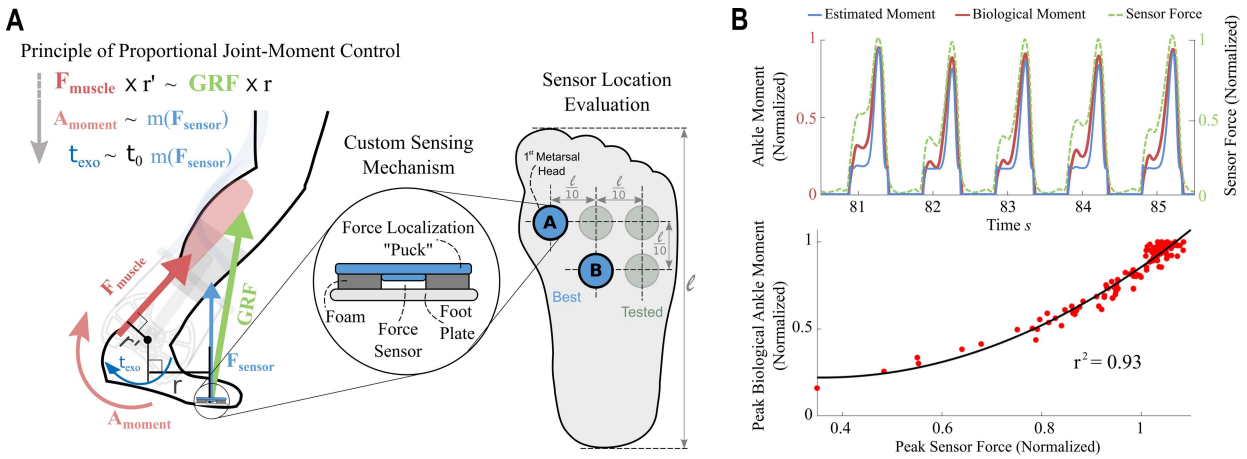

Fig. 2. Theory and development of our proportional joint-moment control strategy. (A) Schematic depiction of the torque balance about the ankle joint that forms basis of proportional joint-moment control (left). Schematic depiction of the evaluated foot sensor locations (right). (B) Comparison of the biological ankle moment and measured sensor forces both normalized by their maximum values during a sensor-calibration trial (top). Scatter plot and 2nd order polynomial regression describing the relationship between peak normalized ankle moment and peak normalized sensor force (bottom).

Next, we developed an equation to relate the instantaneous foot sensor force to the instantaneous ankle joint moment. To do so, we normalized the instantaneous foot sensor force (F_{sen}) by the average peak foot sensor force during a steady-state calibration trail at the preferred walking speed (F_{ref}). This resulted in calculating the instantaneous foot sensor force ratio ($R_F = F_{sen}/F_{ref}$). Finally, we established an equation for estimating the relative instantaneous ankle joint moment by quantifying the relationship between the peaks of the measured foot sensor force ratio (R_F) and the peaks of the normalized biological ankle moment using a 2nd order polynomial regression equation (Fig. 2B, $r^2 = 0.93$), as follows:

$$M_{rel}(t) = 1.29R_F^2 - 0.51R_F + 0.22 \quad (1)$$

where $M_{rel}(t)$ is the instantaneous relative ankle moment normalized by the average peak ankle moment from steady-state walking. Equation (1) constants were established from the regression equation so that the relative ankle moment ($M_{rel}(t)$) was equal to 1 when the instantaneous foot sensor force (F_{sen}) was equal to the foot sensor reference (F_{ref}) (i.e. when $R_F = 1$). Therefore, Equation (1) returned a value for $M_{rel}(t)$ as a fraction of the peak ankle moment during steady-state walking. This approach relied on the following assumptions: 1) the moment arm between the center of force application and the ankle joint was accounted for in the regression equation and normalization process, and 2) the regression equation, developed from one individual, would be suitable for other individuals.

C. Controller Implementation

Proportional joint-moment control was incorporated within a real-time exoskeleton control scheme (Fig. 3). Operation of the controller required a 5-second calibration procedure to determine the foot sensor force reference (F_{ref}) at the user's preferred speed. During calibration, foot sensor

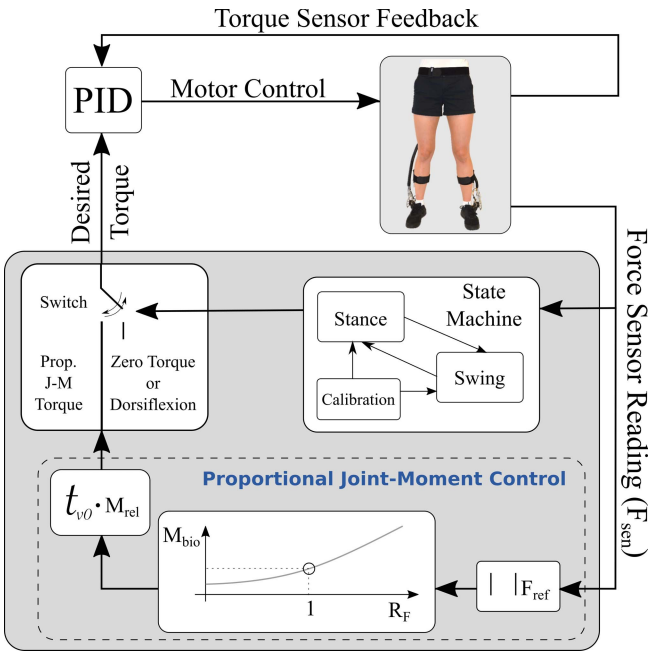

Fig. 3. Real-time control scheme. Implementation of proportional joint-moment control within the exoskeleton control system block diagram.

forces were recorded while each user walked at their preferred steady-state speed with the exoskeleton operating under zero-torque control.

During operation of the controller following calibration, exoskeleton assistance ($\tau(t)$) was provided as a function of the instantaneous relative estimated ankle moment $M_{rel}(t)$, as in Equation (2):

$$\tau(t) = t_{v0} \cdot M_{rel}(t) \quad (2)$$

where τ_{v0} is the reference torque magnitude established for each user at their preferred steady-state walking speed ($v0$). For this study, the reference torque magnitude (τ_{v0}) was

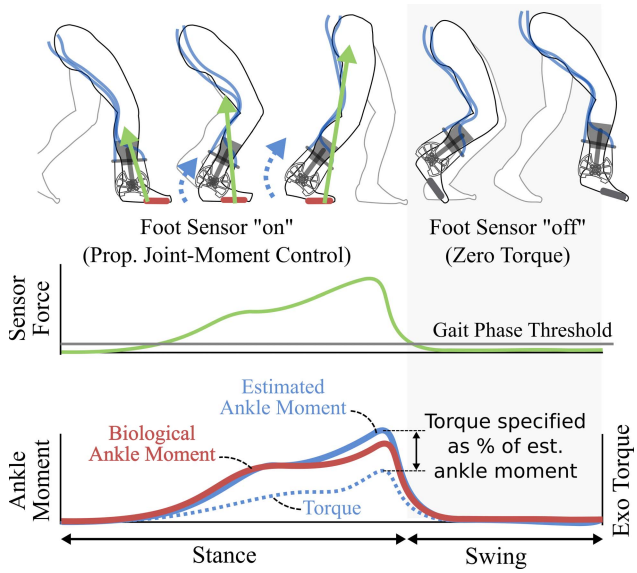

Fig. 4. State machine. Schematic depiction of the state machine and proportional assistance across the gait cycle. The foot sensor "on" state, during which proportional joint-moment control was enacted, occurred from flat-foot to toe-off. The exoskeleton maintained zero-torque at all other times (i.e. during swing and from heel-strike to just prior to flat-foot).

established for each participant based on individual preference within a previously established optimal range [23]. We previously found that 0.20-0.35 Nm/kg of peak plantar-flexor assistance maximized the reduction in metabolic cost of transport while using the device during steady-state walking at preferred speeds. During an "assistance tuning" trial, we initially set the reference torque magnitude (τ_{v0}) at 0.20 Nm/kg, and gradually increased it to the highest level tolerated, up to a maximum of 0.35 Nm/kg. Equal torque was provided across limbs.

As a result of Equation (2), the specified exoskeleton torque adapted instantaneously to the demand placed on the biological joint during walking by prescribing assistance as a fraction of the peak estimated ankle moment during steady-state. When the relative instantaneous ankle moment ($M_{rel}(t)$) was equal to 1, Equation (2) prescribed exoskeleton assistance ($\tau(t)$) that was equal to the user's reference torque magnitude (τ_{v0}); when $M_{rel}(t)$ is not equal to 1, τ_{v0} was scaled accordingly.

Because our primary objective was to provide proportional plantar-flexor assistance during the stance phase, we used a state machine to distinguish between the stance and swing phases of walking using a force sensor threshold (Fig. 4). This allowed for the reliable prescription of zero torque or optional dorsi-flexor assistance to treat drop-foot during the swing phase of walking. Following estimation of the ankle moment and prescription of assistance based on Equation (2), low level torque feedback motor control was used to produce the desired instantaneous torque profile.

We have made the proportional joint-moment control code for the ankle exoskeleton available in supplemental material.

D. Ankle Exoskeleton Platform

We implemented the proportional joint-moment control scheme (Equations (1) and (2)) on an untethered (i.e. battery-powered and wireless) robotic ankle exoskeleton (Fig. 5A). The design of the device was published previously [23]. The ankle exoskeleton was designed to minimize the metabolic burden of adding mass to the lower-extremity by placing the motors and battery at the waist. Bowden cables transmitted the torque from DC motors with integrated planetary gearbox (EC-4pole, Maxon) to custom ankle-foot assemblies. Motors, selected based on participant mass, were rated to provide up to 12, 18, and 24 Nm of peak torque. The ankle foot assemblies were composed of aluminum sheet-metal insoles, torque sensors, torque transmission pulleys, Bowden cable attachment points, aluminum bar-stock lateral supports, and plastic-molded calf attachments. The foot plate assembly articulated in the sagittal plane in order to provide plantar-flexion and dorsi-flexion assistance. Torque sensors mounted at the ankle joint and proportional-integral-derivative (PID) motor control were used to track the instantaneous torque profile.

A custom printed circuit board integrated a micro-controller, motor servo-controllers, sensor connectors, signal processing components, a Bluetooth module, and an on-board Lithium Polymer (Li-Po) battery (910 mAh E-flite 6S). Our real-time control scheme (Fig. 3), operating at 1 kHz, was implemented on a 32-bit ARM microprocessor (Teensy 3.6, TJRC). We created a graphical user interface (GUI) in Matlab to remotely calibrate sensor thresholds, specify torque setpoints, and record experimental data via Bluetooth.

E. Participants and Setup for Experimental Evaluation

This study was approved by the Institutional Review Board at Northern Arizona University (NAU). We sought to assess controller feasibility and accuracy across a range of participant characteristics and a variety of different gait patterns. Three individuals with mild-to-moderate gait deficits from CP, one individual with mild gait deficits from Parkinson's disease, and one unimpaired individual participated in this study (Table I). Participants CP_1, CP_2, and CP_3 exhibited reduced ankle push-off. We obtained written consent from each adult participant, and written parental consent for the child participant. Inclusion criteria included the ability to walk 10m with or without a walking aid; 10 degrees of ankle plantar-flexion passive range of motion; and the absence of any health concern, other than CP or Parkinson's, that would impact safety. Exclusion criteria included orthopedic surgery within 6 months. All visits took place at NAU's Human Performance Laboratory.

On an initial visit, we took measurements for the fabrication of each participant's custom ankle-foot-orthoses (foot-plates, up-rights, and shank cuffs). A physical therapist completed a neuromuscular exam for the participants with CP and Parkinson's disease. Every participant completed at least two training visits during which they practiced walking with nominal exoskeleton assistance.

F. Experimental Validation of Controller Performance

We implemented a treadmill walking task that involved a gait transition profile (gait initiation and variable walking speed) to evaluate the ability of the control algorithm to

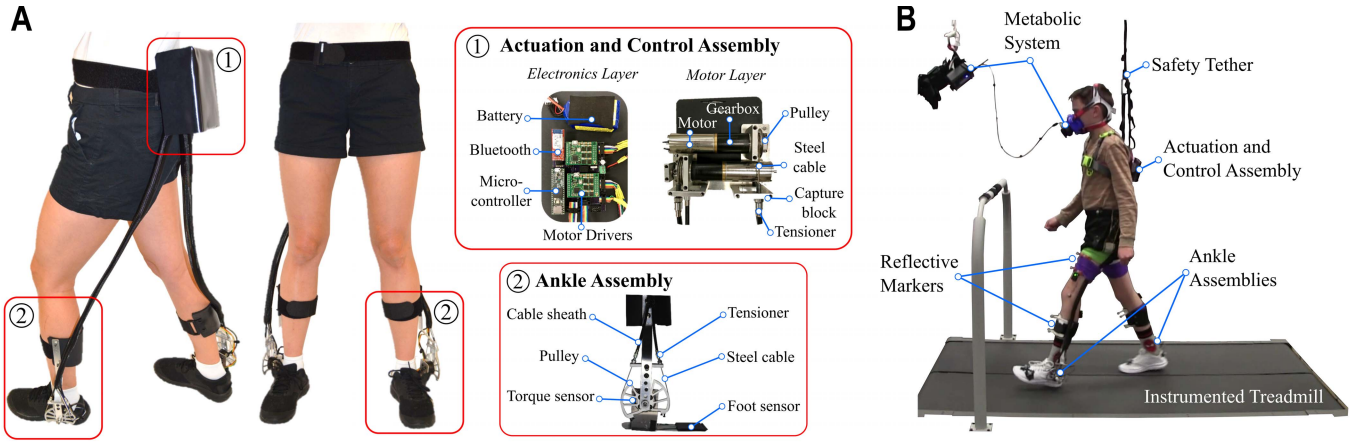

Fig. 5. The ankle exoskeleton and experimental setup. (A) The ankle exoskeleton used in this pilot study was composed of (1) a control and actuation assembly placed above the waist, (2) an ankle assembly, and Bowden cable transmission. (B) Picture of one of the CP participants walking with the exoskeleton during evaluation of gait energetics and biomechanics on an instrumented treadmill.

provide exoskeleton torque proportional to the instantaneous joint moment. First, participants walked for ~60-120 seconds at their preferred speed (v_0) to establish the preferred torque magnitude at that speed (t_{v0}) and calibrate the sensors to obtain the foot sensor force reference (F_{ref}).

For each gait transition task, participants started by standing on the middle of the treadmill at a stand-still. Next, participants were asked to match the treadmill belt speed, which increased at constant acceleration until it reached each participant's preferred speed. Following 10 seconds at the constant preferred speed, the treadmill decreased speed at a constant rate back to a stand-still. We evaluated two relative rates of acceleration/deceleration such that the time from standstill to preferred speed occurred over 10 seconds (faster transition trials) and over 15 seconds (slower transition trials). These intervals were established through observation of safe treadmill acceleration rates in our prior studies of individuals with CP [23], [24]. Each of the two transition tasks were repeated twice. The necessary experimental data were collected to calculate the biological ankle moment during each task. We recorded individual limb ground reaction forces at 960 Hz from the split-belt in-ground instrumented treadmill (Bertec) and retro-reflective marker trajectories at 120 Hz using 10 motion capture cameras (Vicon). As described in [24], marker clusters were placed on each shank and thigh, while individual reflective markers were placed on anatomical landmarks of the feet, ankles, knees, pelvis, and torso of each participant according to recommended standards (Fig. 5B). Marker trajectories and ground reaction forces were low-pass filtered at 6 Hz and 12 Hz, respectively. Participant CP_3 required the use of an overhead handle.

A generic musculoskeletal model was scaled to the anthropometrics of each participant in OpenSim [25]; exoskeleton inertial parameters were included in each scaled model. Joint angles and moments were calculated in OpenSim via inverse kinematics and inverse dynamics, respectively. Because the total joint moment established by inverse dynamics does not distinguish between the biological and exoskeleton contributions, the biological contribution was isolated by subtracting off the measured exoskeleton torque [26]. Desired (i.e. controller-specified) and measured exoskeleton torque data were wirelessly recorded on the exoskeleton control laptop and synchronized with the motion capture system.

To quantify the accuracy of the proportional joint-moment controller, we computed the root-mean-square error (RMSE) between the desired exoskeleton torque normalized by the prescribed level of assistance (t_{v0}) and the biological ankle moment normalized by the peak moment at the preferred speed.

G. Experimental Evaluation of Metabolic Benefit

A secondary goal of this paper was to provide preliminary evidence that our proportional joint-moment control strategy was effective in improving walking economy for individuals with and without neuromuscular gait disorders. We measured metabolic energy expenditure while the three most ambulatory participants completed steady-state walking trials. To assess the effects of proportional joint-moment control isolated from changes in walking speed and allow for comparison to prior studies, participants CP_1 and U_5 completed steady-state walking trails on a treadmill at their preferred (fixed) speed. We also sought to provide initial evidence of controller effectiveness in a more realistic freely-living setting. Therefore, participant CP_2 completed an over-ground walking trial on a rectangular track (17 m × 23 m) while he self-selected his speed.

For these steady-state trials, participants completed two conditions: (1) walking with the exoskeleton providing torque via proportional joint-moment control and (2) walking with the exoskeleton operating under zero-torque control. For this evaluation designed to provide initial evidence of the ability of proportional joint-moment control to improve walking efficiency, comparison was made to the zero-torque control condition to isolate the effects of the controller independent of device mass. We previously demonstrated the ability of our zero-torque controller to accurately compensate for friction and motor inertia [23]. Testing order was randomized across participants. Trials lasted for a minimum of six minutes. Metabolic

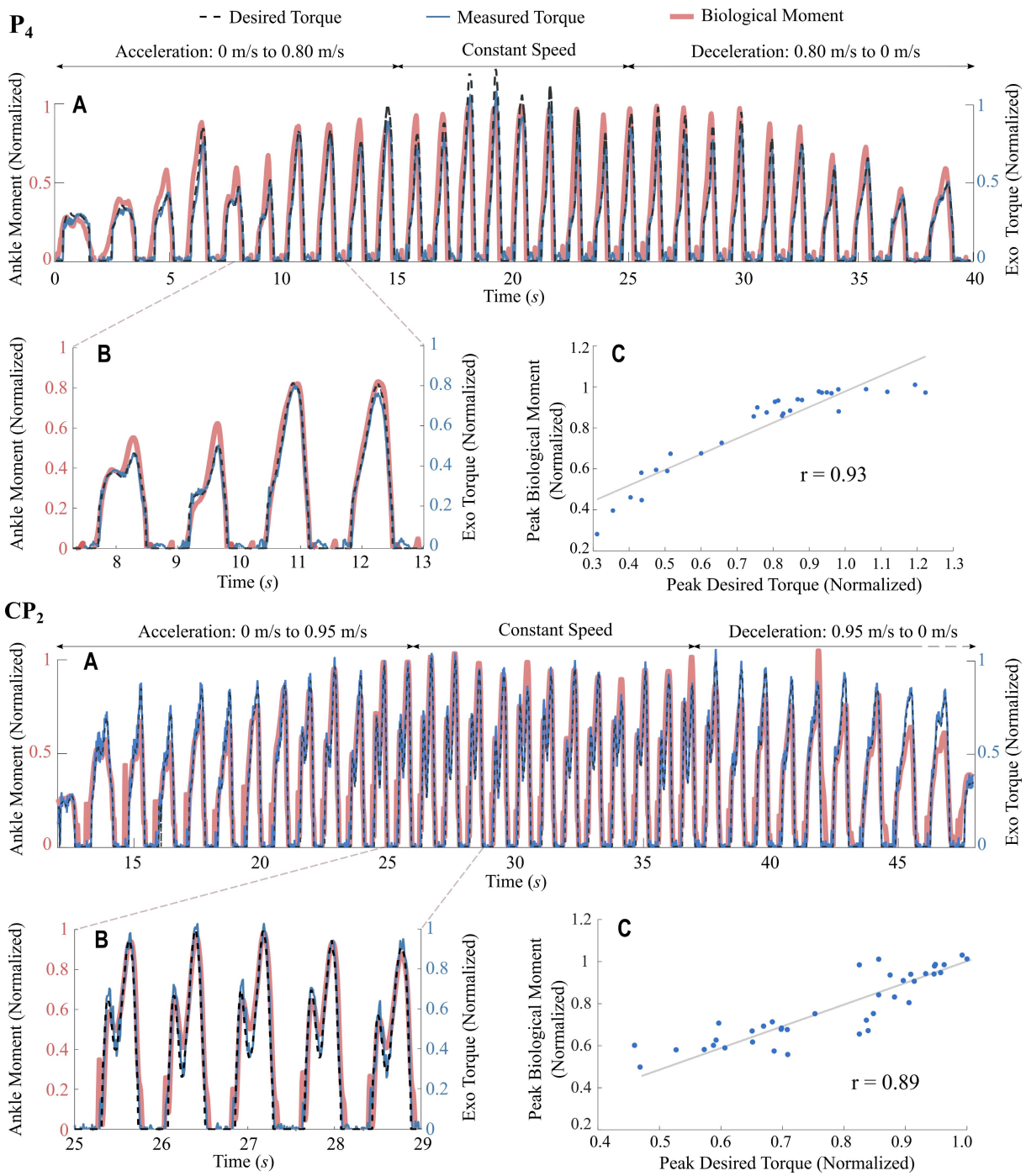

Fig. 6. Comparison of biological ankle moment and proportional joint-moment controller-specified torque during gait transition validation trials. (A) Biological ankle moment (red), and proportional joint-moment controller prescribed (black, dashed) and measured (blue) exoskeleton torque across an entire representative gait transition trial for P_4 (top) and CP_2 (bottom). To help visual controller accuracy, ankle moments were normalized by the peak ankle moment during each participant's calibration trail at preferred speed, while the exoskeleton torques were normalized by the nominal preferred torque value at preferred speed; complete overlap indicates perfect accuracy. In absolute terms, the exoskeleton torque was providing approximately 1/3rd of the total (exoskeleton component plus biological component) ankle moment. (B) Expanded view from each gait transition trial depicting regions of high controller accuracy. (C) The relationship between the peak normalized biological ankle moment and peak normalized exoskeleton torque during the gait cycle from each presented gait transition trial.

data were recorded using a portable metabolic system (K5, Cosmed) and averaged over the final minute. Metabolic cost was computed from measurements of oxygen consumption (VO_2) and carbon dioxide production ($VC0_2$) according to the standard Brockway equation [27]. Net metabolic cost was computed by subtracting the baseline metabolic rate of quiet standing from the metabolic rate during walking. Net metabolic cost of transport was computed by normalizing net metabolic cost by the average walking speed of each trial.

TABLE II
CONTROLLER PERFORMANCE BY GAIT TRANSITION PHASE

Trial	Acceleration Phase	Constant Velocity Phase	Deceleration Phase
Slower	13.3 ± 3.4	14.8 ± 4.8	13.4 ± 3.5
Faster	12.8 ± 4.1	13.9 ± 5.5	12.2 ± 4.6

Values are mean ± standard deviation

III. RESULTS

A. Controller Performance During Gait Transitions

Our proportional joint-moment controller was effective in estimating the stance-phase biological ankle moment in real-time, which varied considerably, up to 77% of the peak, across the walking transition task (Fig. 6). In general, the ankle moment increased during the acceleration phase and decreased during the deceleration phase. The desired torque profile specified from the proportional joint-moment controller closely matched the timing, shape, and magnitude of the computed ankle moment (Fig. 6). Across both acceleration tasks, the average stance-phase RMSE between the controller's normalized prescribed assistance (i.e. estimated moment) and the computed ankle moment was 13.5 ± 4.0% (Fig. 7); RMSE for the acceleration, constant-velocity, and deceleration phases of both gait transition tasks were between 12.8% and 14.8% (Table II). The error between the predicted and measured ankle moment was largest (22.8%) for the participant with the greatest gait impairment (CP_3, GMFCS III), and lowest (8.1%) for the participant with Parkinson's disease (P_4). The average stance-phase RMSE between the measured exoskeleton torque output and the desired (i.e. controller-specified) profile torque was 6.0 ± 0.5% (Fig. 7). The average stance-phase RMSE between the normalized measured exoskeleton torque output and the normalized biological ankle moment was 13.1 ± 4.0% across both acceleration tasks.

B. Metabolic Cost During Steady-State Walking Trials

We found that proportional joint-moment control was effective in reducing the metabolic cost of walking (Fig. 8A). Compared to walking without assistance, participant CP_1 and U_5 exhibited 18.3% and 26.5% reductions in metabolic cost of transport, respectively, during treadmill walking with proportional joint-moment control at their constant preferred speeds. Participant CP_2 exhibited a 17.3% reduction in metabolic cost of transport during over-ground walking at his self-selected speed.

IV. DISCUSSION

The primary goal of this study was to design and validate an ankle exoskeleton control algorithm that automatically adjusts assistance during variable walking conditions while maximizing clinical usability outside of controlled research environments. To meet this goal, we designed, tested, and clinically evaluated a proportional joint-moment controller that adapts instantaneously to the biological demand placed on the ankle joint. Tested during "slow" and "fast" gait transitions, the control scheme was able to match the timing, shape, and magnitude of the biological ankle moment to within 14% error. Preliminary testing of proportional joint-moment control during both treadmill and over-ground steady-state walking demonstrated that this control scheme is effective in reducing the metabolic cost of transport between 17-27% relative to an unassisted condition. This work supports our long-term goal of utilizing wearable exoskeletons to improve free-living mobility for ambulatory individuals with neuro-motor impairment, and contributes to a growing body work related to ground reaction force estimation-based control of powered lower-extremity prosthetics [28].

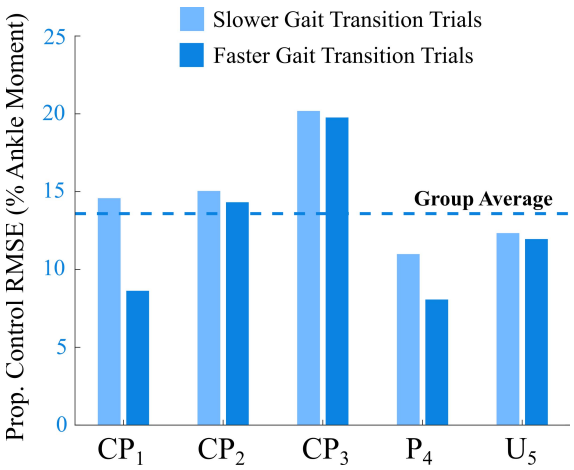

Fig. 7. Proportional joint-moment controller performance. RMSE between the proportional joint-moment controller's normalized prescribed assistance and the biological ankle moment during the slower (light blue) and faster (dark blue) gait transition trials for each participant. The narrow dark and light gray bars depict the RMSE between the desired and measured exoskeleton torque (PID torque tracking error).

The gait transition trials implemented in this study elicited wide-ranging ankle joint moment magnitudes, with a dynamic range of ~75% relative to steady-state walking maximums. Moreover, the participants exhibited vastly different walking patterns, including unimpaired gait, mild-moderate crouch gait and mild Parkinsonian gait. Despite these challenging conditions, our proportional joint-moment controller wasable to predict the ankle moment in real-time with high fidelity. Still, the regression equation used to estimate the ankle moment from the foot sensor forces was developed using walking data collected from a single unimpaired individual. Inclusion of a larger training dataset would likely increase the controller accuracy.

Eliciting an improvement in the metabolic cost of walking with robotic assistance can be difficult to achieve, even on a treadmill, as it requires the highly-personalized synergistic timing and level of assistance. We previously demonstrated that finely-tuned on-off control can be used to improve walking economy during treadmill walking in individuals with CP [23]. The present study demonstrates that proportional joint-moment control is similarly effective during treadmill walking. An objectively greater challenge seems to be utilizing powered exoskeletons to improve the energy cost of over-ground walking, which likely requires assistance that adapts to the user's subtle changes in self-selected speed. To the best of our knowledge, this is the first study to demonstrate a reduction in metabolic cost of transport during

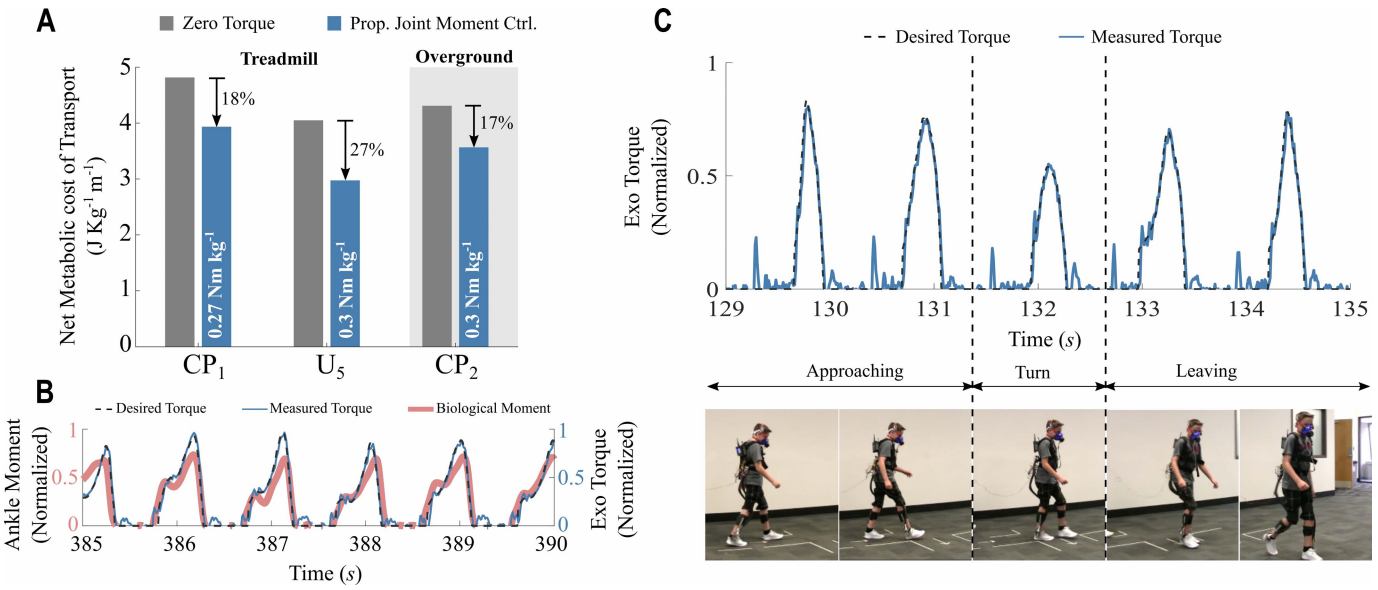

Fig. 8. Metabolic cost of transport during steady-state walking. (A) Reduction in metabolic cost of transport during treadmill and over-ground walking with proportional joint-moment control (blue) compared to zero-torque control (green). (B) Comparison of normalized biological ankle joint moment (red), desired (black, dashed), and measured (blue) exoskeleton torque during walking with proportional joint-moment control across several representative gait cycles from the steady-state treadmill walking trial for CP_1. (C) Desired (black, dashed) and measured torque as participant CP_2 approached and departed a right-hand turn during the steady-state over-ground walking trial with proportional joint-moment control.

over-ground walking with a wearable ankle exoskeleton, made possible by the instantaneous adaptability of proportional joint-moment control (one study has demonstrated improved efficiency for unimpaired over-ground walking with hip extension assistance from a soft exosuit [29]). Motion capture, and therefore comparison of the predicted and calculated ankle moment, was not available during the over-ground walking trials. However, our observations were consistent with expected changes in assistance across the rectangular over-ground walking path. For example, we observed a reduction in exoskeleton torque application as a result of lower predicted ankle moment when the participant slowed to encounter each turn (Fig. 8C).

Proportional joint-moment control may become a promising alternative to other control strategies designed to provide adaptive assistance. Control of exoskeleton assistance using muscle activity via proportional myoelectric control has been well established as an effective control scheme during walking by unimpaired individuals [14], [15], [30], as it offers the ability to detect the user's intent. For individuals with neuromotor impairment suffering from muscle spasticity, proportional myoelectric control may not be effective or desirable because muscle spasticity likely obscures or saturates the neural signal [16]. Proportional joint-moment control cannot directly sense the user's intent for feed-forward control. However, by adapting to the dynamics of biological joints in real-time, the controller, in effect, senses the net result of the neural commands. Indeed, the perception from our study participants was that the exoskeleton responded directly to their intended actions. Intent recognition and activity classification are other approaches designed to provide assistance that meet the demands of different walking conditions [20], [21]. An advantage of proportional control strategies, like proportional joint-moment control, is that they do not require additional classifier training for unique and asymmetric pathological gait patterns. Additionally, proportional joint-moment control prevents the potentially dangerous application of mismatched torque that can occur with misclassification.

We anticipate that the proportional joint-moment controller outlined in this study is well suited for real-world application and adoption. Because the force sensors necessary for proportional joint-moment control are embedded in the exoskeleton's foot plates, no addition sensors, components, or adjustments are needed once the exoskeleton has been fitted to the user, resulting in minimal set-up time and low burden of use. Proportional joint-moment control is intuitive and simple to understand for young or cognitively impaired participants. It allows for direct user input and testing (i.e. pressing harder will increase assistance, and vice-versa). Exoskeleton calibration can be quickly and easily self-implemented; upon donning the device each session, the user could simply tune the amount of assistance to preference while walking at their normal speed before entering into proportional control.

We evaluated the control scheme during level walking in a straight line, focusing on arguably the most common yet simple gait transition encountered during daily life. Therefore, the accuracy of the control algorithm during turning and sloped walking is unknown. A future validation study will focus on evaluating the performance of the controller across different locomotor tasks, including incline and decline walking, and stair ascent and descent. While a strength of this study was the heterogeneous patient population that spanned the range of walking abilities (unimpaired to moderate/severe impairment), additional research is needed to determine whether proportional joint-moment control will be a suitable approach for individuals who are unable to walk independently. Our future work will also focus on assessing the effects of

proportional joint-moment control on additional clinical outcomes, including gait mechanics and balance.

User preference and perception of benefit are important aspects that should be considered for compliance and real-world adoption of wearable assistive devices. The direct comparison of subject preference between exoskeleton control schemes was outside the scope of this feasibility study. However, some of the participants in the present study previously walked with our non-adaptive but finely-tuned control scheme that was effective in reducing the metabolic cost of walking in individuals with CP [23]. When asked which exoskeleton controller was preferred, all of the participants responded vehemently in favor of proportional joint-moment control; this was an anecdotal but very encouraging finding that must be studied more rigorously in the future.

In conclusion, we designed, tested, and clinically evaluated an ankle exoskeleton controller that provides assistance proportional to the instantaneous ankle moment. We validated controller performance during a gait transition task and found that the controller was able to provide assistance proportional to the ankle moment in a diverse cohort of ambulatory individuals with and without neuromotor walking disorders. We also presented preliminary evidence on the efficacy of proportional joint-moment control to improve treadmill and over-ground walking economy in impaired and unimpaired individuals. The next critical step for evaluation of this novel control strategy will be to determine if proportional joint-moment control reduces metabolic cost of transport compared to how individuals walk without wearing the exoskeleton, evaluated in a larger clinical population. We anticipate that the ease and simplicity of the controller is well-suited for use outside of the laboratory. Ultimately, this work supports our ongoing efforts in conducting exoskeleton intervention studies that seek to improve mobility for individuals with walking disorders at home and in the community.

Acknowledgment

The authors thank Taryn Harvey, Jenny Lawson, and Leah Liebelt for their assistance with this study.

References

[1] A. Opheim, R. Jahnsen, E. Olsson, and J. K. Stanghelle, "Walking function, pain, and fatigue in adults with cerebral palsy: A 7-year follow-up study," *Develop. Med. Child Neurol.*, vol. 51, no. 5, pp. 381–388, 2009.

[2] S. R. Hilberink, M. E. Roebroeck, W. Nieuwstraten, L. Jalink, J. M. A. Verheijden, and H. J. Stam, "Health issues in young adults with cerebral palsy: Towards a life-span perspective," *J. Rehabil. Med.*, vol. 39, no. 8, pp. 605–611, 2007.

[3] T. A. Boonstra, H. Van Der Kooij, M. Munneke, and B. R. Bloem, "Gait disorders and balance disturbances in Parkinson's disease: Clinical update and pathophysiology," *Current Opinion Neurol.*, vol. 21, no. 4, pp. 461–471, 2008.

[4] Centers for Disease Control and Prevention, "Outpatient rehabilitation among stroke survivors–21 States and the District of Columbia, 2005," *MMWR. Morbidity Mortality Weekly Rep.*, vol. 56, no. 20, pp. 504–507, 2007.

[5] K. F. Bjornson, B. Belza, D. Kartin, R. Logsdon, and J. F. McLaughlin, "Ambulatory physical activity performance in youth with cerebral palsy and youth who are developing typically," *Phys. Therapy*, vol. 87, no. 3, pp. 248–257, 2007.

[6] S. H. J. Keus, M. Munneke, M. J. Nijkrake, G. Kwakkel, and B. R. Bloem, "Physical therapy in Parkinson's disease: Evolution and future challenges.," *Movement Disorders*, vol. 24, no. 1, pp. 1–14, 2009.

[7] C. L. Brockett and G. J. Chapman, "Biomechanics of the ankle," *Orthopaedics Trauma*, vol. 30, no. 3, pp. 232–238, 2016.

[8] T.-W. P. Huang, K. A. Shorter, P. G. Adamczyk, and A. D. Kuo, "Mechanical and energetic consequences of reduced ankle plantarflexion in human walking," *J. Exp. Biol.*, vol. 218, no. 22, pp. 3541–3550, 2015.

[9] T. F. Winters, Jr., J. R. Gage, and R. Hicks, "Gait patterns in spastic hemiplegia in children and young adults," *J. Bone Joint Surg.*, vol. 69, no. 3, pp. 437–441, 1987.

[10] D. J. Villarreal and R. D. Gregg, "A survey of phase variable candidates of human locomotion," in *Proc. 36th Annu. Int. Conf. IEEE Eng. Med. Biol. Soc. (EMBC)*, Aug. 2014, pp. 4017–4021.

[11] D. Quintero, A. E. Martin, and R. D. Gregg, "Toward unified control of a powered prosthetic leg: A simulation study," *IEEE Trans. Control Syst. Technol.*, vol. 26, no. 1, pp. 305–312, Jan. 2018.

[12] R. J. Farris, H. A. Quintero, and M. Goldfarb, "Performance evaluation of a lower limb exoskeleton for stair ascent and descent with Paraplegia," in *Proc. Annu. Int. Conf. IEEE Eng. Med. Biol. Soc. (EMBC)*, Aug./Sep. 2012, pp. 1908–1911.

[13] B. H. Hu, E. J. Rouse, and L. J. Hargrove, "Using bilateral lower limb kinematic and myoelectric signals to predict locomotor activities: A pilot study," in *Proc. Int. IEEE/EMBS Conf. Neural Eng. (NER)*, May 2017, pp. 98–101.

[14] D. P. Ferris and C. L. Lewis, "Robotic lower limb exoskeletons using proportional myoelectric control," in *Proc. 31st Annu. Int. Conf. IEEE Eng. Med. Biol. Soc. (EMBC)*, Sep. 2009, pp. 2119–2124.

[15] G. S. Sawicki and D. P. Ferris, "Mechanics and energetics of level walking with powered ankle exoskeletons," *J. Experim. Biol.*, vol. 211, no. 9, pp. 1402–1413, 2008.

[16] V. Dietz, "Proprioception and locomotor disorders," *Nature Rev. Neurosci.*, vol. 3, pp. 781–790, Oct. 2002.

[17] K. S. Türker, "Electromyography: Some methodological problems and issues," *Phys. Therapy*, vol. 73, no. 10, pp. 698–710, 1993.

[18] D. Farina, "Interpretation of the surface electromyogram in dynamic contractions," *Exerc. Sport Sci. Rev.*, vol. 34, no. 3, pp. 121–127, 2006.

[19] J. Zhang *et al.*, "Human-in-the-loop optimization of exoskeleton assistance during walking," *Science*, vol. 356, no. 6344, pp. 1280–1283, 2017.

[20] H. Kawamoto, S. Kanbe, and Y. Sankai, "Power assist method for HAL-3 estimating operator's intention based on motion information," in *Proc. 12th IEEE Int. Workshop Robot Hum. Interact. Commun.*, Nov. 2003, pp. 67–72.

[21] Y. D. Li and E. T. Hsiao-Wecksler, "Gait mode recognition and control for a portable-powered ankle-foot orthosis," in *Proc. 13th IEEE Int. Conf. Rehabil. Robot.*, Jun. 2013, pp. 1–8.

[22] L. Lonini, A. Gupta, S. Deems-Dluhy, S. Hoppe-Ludwig, K. Kording, and A. Jayaraman, "Activity recognition in individuals walking with assistive devices: The benefits of device-specific models," *JMIR Rehabil. Assistive Technol.*, vol. 4, no. 2, p. e8, 2017.

[23] Z. F. Lerner *et al.*, "An untethered ankle exoskeleton improves walking economy in a pilot study of individuals with cerebral palsy," *IEEE Trans. Neural Syst. Rehabil. Eng.*, vol. 26, no. 10, pp. 1985–1993, Oct. 2018.

[24] Z. F. Lerner, D. L. Damiano, and T. C. Bulea, "A lower-extremity exoskeleton improves knee extension in children with crouch gait from cerebral palsy," *Sci. Transl. Med.*, vol. 9, no. 404, 2017, Art. no. eaam9145.

[25] S. L. Delp *et al.*, "OpenSim: Open-source software to create and analyze dynamic simulations of movement," *IEEE Trans. Biomed. Eng.*, vol. 54, no. 11, pp. 1940–1950, Nov. 2007.

[26] K. Shamaei, M. Cenciarini, A. A. Adams, K. N. Gregorczyk, J. M. Schiffman, and A. M. Dollar, "Biomechanical effects of stiffness in parallel with the knee joint during walking," *IEEE Trans. Biomed. Eng.*, vol. 62, no. 10, pp. 2389–2401, Oct. 2015.

[27] J. M. Brockway, "Derivation of formulae used to calculate energy expenditure in man.," *Hum. Nutrition. Clin. Nutrition*, vol. 41, no. 6, pp. 463–471, 1987.

[28] V. Azimi, T. T. Nguyen, M. Sharifi, S. A. Fakoorian, and D. Simon, "Robust ground reaction force estimation and control of lower-limb prostheses: Theory and simulation," *IEEE Trans. Syst., Man, Cybern. Syst.*, to be published.

[29] J. Kim *et al.*, "Autonomous and portable soft exosuit for hip extension assistance with online walking and running detection algorithm," in *Proc. IEEE Int. Conf. Robot. Automat. (ICRA)*, May 2018, pp. 1–8.

[30] D. P. Ferris, K. E. Gordon, G. S. Sawicki, and A. Peethambaran, "An improved powered ankle–foot orthosis using proportional myoelectric control," *Gait Posture*, vol. 23, no. 4, pp. 425–428, 2006.